ELSEVIER

Journal of Hazardous Materials 140 (2007) 173–179

Journal of Hazardous Materials

www.elsevier.com/locate/jhazmat

Modification of bentonite with a cationic surfactant: An adsorption study of textile dye Reactive Blue 19

Adnan Özcan [a,*], Çiğdem Ömeroğlu [b], Yunus Erdoğan [b], A. Safa Özcan [a]

[a] *Department of Chemistry, Faculty of Science, Anadolu University, Yunusemre Campus, 26470 Eskişehir, Turkey*
[b] *Department of Chemistry, Faculty of Arts and Science, Dumlupinar University, Kutahya, Turkey*

Received 28 March 2006; received in revised form 16 June 2006; accepted 19 June 2006
Available online 10 July 2006

Abstract

The utilization of modified bentonite with a cationic surfactant (dodecyltrimethylammonium (DTMA) bromide) as an adsorbent was successfully carried out to remove a synthetic textile dye (Reactive Blue 19 (RB19)) by adsorption, from aqueous solutions. Batch studies were carried out to address various experimental parameters such as pH, contact time and temperature. The surface modification of bentonite with a surfactant was examined using the FTIR spectroscopic technique and elemental analysis. Effective pH for the adsorption of RB19 onto DTMA–bentonite was around 1.5. The Langmuir isotherm model was found to be the best to represent the equilibrium with experimental data. The maximum adsorption capacity (q_{max}) has been found to be 3.30×10^{-4} mol g^{-1} or 206.58 mg g^{-1}. The thermodynamic study indicated that the adsorption of RB19 onto DTMA–bentonite was favored with the negative Gibbs free energy values. The pseudo-second-order rate equation was able to provide the best description of adsorption kinetics and the intraparticle diffusion model was also applicable up to 40 min for the adsorption of RB19 onto DTMA–bentonite.

Keywords: Bentonite; Organoclay; Adsorption; Reactive dye; Isotherms

1. Introduction

Large volumes of colored aqueous effluents are discharged by the various sectors, such as textiles, leather, printing, laundry, tannery, rubber, plastic, painting, etc., industries [1]. The presence of very low concentrations of these effluents are highly visible and undesirable and potentially inhibiting photosynthesis. Owing to their chemical structure, dyes are resistant to fading when exposed to light, water and chemicals [2]. Reactive dyes are the most widely used dyes in the textile industry. These types of dyes are colored compounds that have highly soluble in water and have reactive groups which are able to form covalent bonds between dye and fiber [3]. Untreated disposal of this colored water into receiving water body causes damage to aquatic life and also it severe damages to the human bodies [4–6].

The removal of color from dye-house wastewater is currently one of the major problems faced by the textile dyeing industry. Various physical, chemical and biological treatment methods have been used for the treatment of these textile effluents. However, these methods have certain disadvantages such as high capital cost and operational costs or secondary sludge disposal problems. Instead of these methods, the adsorption technique can be applied to remove these kinds of textile effluents. Adsorption offers significant advantages over traditional treatment methods especially environmental point of view [7–13]. Although activated carbon is widely used as an adsorbent for dye removal from colored waters owing to its excellent adsorption abilities, it is high price, which limits their usage [14,15]. Hence, alternative low-cost, novel, locally available adsorbents are currently used for the removal of textile dye effluents from aqueous solutions, instead of activated carbon. For instance, clays such as sepiolite [5,6,8,16], zeolite [17–20], montmorillonite [21–23], smectite [24–26] and bentonite [14,15,27,28] can be used in these respects.

One of the clay minerals, which is namely bentonite, is composed of units made up of two silica tetrahedral sheets with a

* Corresponding author. Tel.: +90 222 3350580/5815; fax: +90 222 3204910.
E-mail addresses: aozcan@anadolu.edu.tr (A. Özcan), cigdem@dumlupinar.edu.tr (Ç. Ömeroğlu), yerdogan@dumlupinar.edu.tr (Y. Erdoğan), asozcan@anadolu.edu.tr (A.S. Özcan).

0304-3894/$ – see front matter © 2006 Elsevier B.V. All rights reserved.
doi:10.1016/j.jhazmat.2006.06.138

central Al octahedral sheet. It has permanent negative charges that increase owing to the isomorphous substitution of Al^{3+} for Si^{4+} in the tetrahedral layer and Mg^{2+} for Al^{3+} in the octahedral layer. This negative charge is balanced by the presence of exchangeable cations (Na^+, Ca^{2+}, etc.) in the lattice structure. Acid and reactive dyes are water soluble anionic dyes are negatively charged and are used to dye textile fibres. Due to the fact that the anionic dyes are negatively charged, the surface of the natural clays has to be modified by a cationic surfactant for the dye adsorption experiments. By the ion-exchange mechanism, the inorganic cation could be exchanged by the organic surfactant cation. Thus, this modification is termed as organoclay and the introduction of organic cation changes the clay from hydrophilic to hydrophobic form. As a result, the adsorption capacity of organoclay increases to compare with natural clay mineral and it can be used as an adsorbent for the adsorption of dyes [15,29,30].

The characteristics of the dye adsorption behavior are mainly understood in terms of the equilibrium isotherms, thermodynamic parameters and adsorption kinetics. The aim of the present work is to study the adsorption capacity of surfactant-modified bentonite for a dye (Reactive Blue 19, RB19), which is an anionic dye, removal from aqueous solutions. The experimental data for adsorbed RB19 onto surfactant-modified bentonite were compared using two isotherm equations, which are Langmuir and Freundlich. The equilibrium thermodynamic parameters are also determined for the RB19 onto surfactant-modified bentonite. Finally, two kinetic models, which are the pseudo-second-order and intraparticle diffusion, were tested in this study.

2. Materials and methods

A commercial textile dye Reactive Blue 19 (RB19) (Remazol Brilliant Blue R) (C.I. 61200) was provided from Bursa, Turkey and used in all adsorption experiments without further purification. The chemical structure of RB19 is illustrated in Fig. 1. The natural bentonite was obtained from Çanakkale, Turkey. It was crushed, ground, sieved through a 63-μm sieve, and then dried at 110 °C in a laboratory oven for 2 h prior to use.

Bentonite was characterized with respect to cation exchange capacity (CEC), by ammonium acetate method and the surface area by using surface area analyzer and N_2 gas was used as adsorbate. Dodecyltrimethylammonium (DTMA) bromide was used as a cationic surfactant for the dye adsorption experiments. The Na-exchanged form of bentonite and DTMA modified bentonite were prepared according to the literature [15].

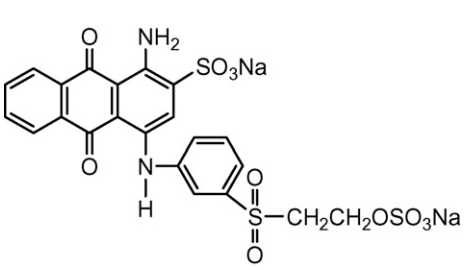

Fig. 1. Chemical structure of RB19.

The chemical analysis of natural bentonite was carried out by using an energy dispersive X-ray spectrometer (EDX-LINK ISIS 300) attached to a scanning electron microscope (SEM-Cam Scan S4).

FTIR spectra for Na–bentonite and DTMA–bentonite were recorded (KBr) on a Jasco FT/IR-300E Model Fourier transform infrared spectrometer to confirm the surface modification.

The elemental analysis (Vario EL III Elemental Analyzer, Hanau, Germany) was performed to determine C/N ratio in DTMA–bentonite.

The pH of each solution was measured by using a laboratory scale pH meter (Fisher Accumet AB15) and the absorbance measurements were carried out on UV–vis spectrophotometer (Shimadzu UV-2101PC) at the respective λ_{max} value (592 nm for RB19).

Adsorption experiments with DTMA–bentonite were performed by batch technique at 20, 30 and 40 °C temperatures. A series of 100 ml Erlenmeyer flasks containing 50 ml of adsorbate solutions of various concentrations ((2.00–4.50) $\times 10^{-4}$ mol dm^{-3}) and required amount of DTMA–bentonite were employed at a desired pH by adding a small amount of HCl or NaOH solutions and temperature. These flasks were closed with parafilm to avoid evaporation and then were stirred using a mechanical magnetic stirrer for 60 min to achieve equilibration, however, stirring for extra 2 h gave practically the same uptake in each case. Once the equilibrium is through to be reached, solution was carefully filtered and concentration of the dye in the solution after equilibrium adsorption was determined spectrophotometrically by measuring the absorbance. The wavelength was recorded before and after the adsorption and in all the cases no shift in the absorbance peak (λ_{max} = 592 nm) was observed.

For kinetic studies 50 ml solution of RB19 of 2.00×10^{-4} mol dm^{-3} concentration and 0.030 g of adsorbent were taken in a 100 ml Erlenmeyer flask. Keeping flask in a water bath, maintained at desired temperature, mixture was mechanically stirred. After a definite interval of time, the solution in the flask was filtered and filtrate of each was analyzed for the uptake of dye.

3. Results and discussion

3.1. Chemical composition of bentonite

The chemical composition and surface area of bentonite and DTMA–bentonite are given in Table 1. As it can be easily seen from Table 1, the major constituents in bentonite are silica and alumina and the impurities are potassium, calcium, magnesium, iron, titanium and sodium oxides. XRD results combined with EDX analysis indicate that most of the aluminum is in the form of bentonite. XRD also indicated the presence of free quartz in bentonite. As a result, it is expected that the adsorbate species will be removed mainly by silica or alumina.

The ratio of C/N for modified-bentonite was obtained from elemental analysis results is 12.61 and the calculated value of C/N ratio for DTMA is 12.86 and the percentage of DTMA onto bentonite is 16.07. These results confirm that the inter-

Table 1
Chemical composition of bentonite

Constituents	Percentage (%)	Cation exchange capacity (CEC)	Specific surface area N_2 atmosphere ($m^2\ g^{-1}$)
SiO_2	70.75	145.74 mequiv./100 g	Bentonite: 35.09; DTMA–bentonite: 32.86
Al_2O_3	16.18		
K_2O	2.12		
CaO	1.62		
MgO	1.25		
Fe_2O_3	0.70		
TiO_2	0.18		
Na_2O	0.11		
Loss of ignition	6.63		

calation of DTMA molecules between the bentonite layers occurs.

FTIR spectra of natural bentonite and DTMA–bentonite are depicted in Fig. 2. A pair of strong bands at 2856 and 2929 cm^{-1} was only observed DTMA–bentonite. They can be assigned to the symmetric and asymmetric stretching vibrations of the methyl and methylene groups and their bending vibrations are between 1396 and 1486 cm^{-1}, supporting the intercalation of DTMA molecules between the silica layers, but these stretching and bending bands are not observed in the natural bentonite. This may be acceptable evidence for the surface modification occurring on bentonite. The band intensities were decreased with surfactant modification of bentonite around at 3400 cm^{-1} (stretching band of the OH groups) and at 1600 cm^{-1} (related to zeolitic water) (see Fig. 2). This is also the evidence for the modification of bentonite with surfactant (DTMA). At the same time, all above FTIR results are consistent with elemental analysis results.

3.2. Adsorption dynamics

Adsorption of RB19 onto DTMA–bentonite was carried out for the examination of the effect of pH at a range of 1–9 and it was found that the adsorption decreased with an increase in pH; as it can be seen from Fig. 3. The variation in the removal of RB19 with respect to pH can be explained by considering the surface charge of the adsorbent. The higher adsorption capacity of the dye onto DTMA–bentonite at low pH values may be due to neutralization of the negative charge at its surface as $–SO_3^-$ anion, which increases the protonation and the other words, increasing the electrostatic attraction between the negatively charged $–SO_3^-$ anion and the positively charged adsorption site. The reason for the high adsorption capacity at low pH is due to the strong electrostatic interaction between the cationic surfactant head groups and dye anions.

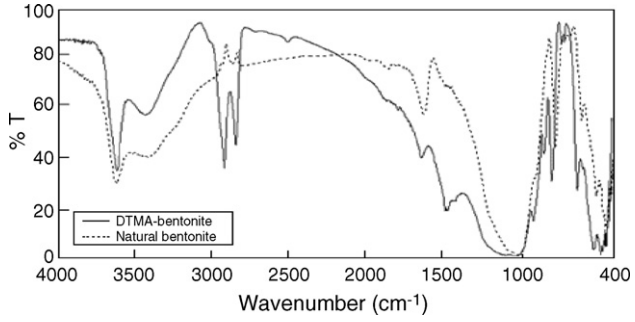

Fig. 2. FTIR spectra of natural bentonite and DTMA–bentonite.

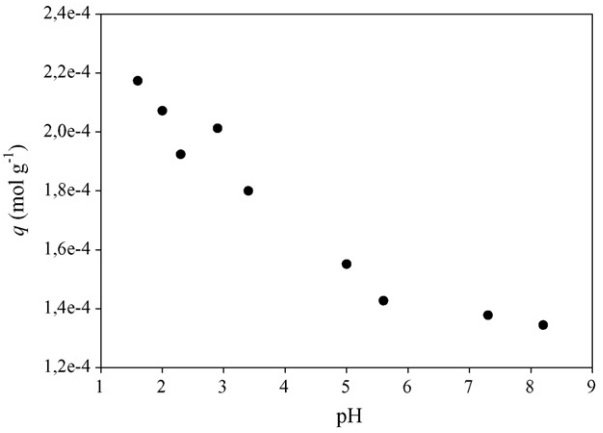

Fig. 3. pH effect for the adsorption of RB19 onto DTMA–bentonite at 20 °C.

Decrease in the dye adsorption capacity with increasing pH may be due to the positive charge on the oxide or solution surface appears negatively charged OH^- ions and the facilities leads to ionic repulsion between the negatively charged surface and the anionic dye molecules. At higher pH values are also not exchangeable anions on the outer surface of the adsorbent and consequently the adsorption capacity decreases. The maximum adsorption capacity of the RB19 takes place at around acidic pH 1.5, which was therefore selected for all further adsorption experiments.

Fig. 4 shows the removal of RB19 by DTMA–bentonite at various adsorbent doses (0.015–0.040 g) for the volume of 50 ml, at the dye concentration 2.00×10^{-4} mol dm^{-3}. It is evident from the figure that as the amount of adsorbent dosage increases up to 0.030 g, the maximum dye removal was attained with this amount and it was used for further experiments.

The adsorption capacity of RB19 removed by DTMA–bentonite versus contact time is illustrated in Fig. 5. It can be seen from this figure that the adsorption capacity of RB19 ions

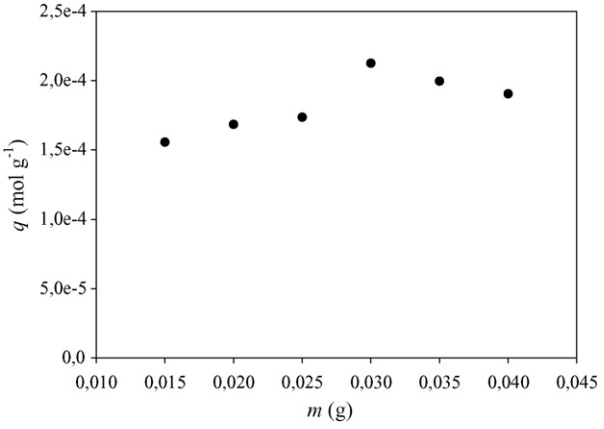

Fig. 4. The effect of adsorbent doses for the adsorption of RB19 onto DTMA–bentonite at 20 °C.

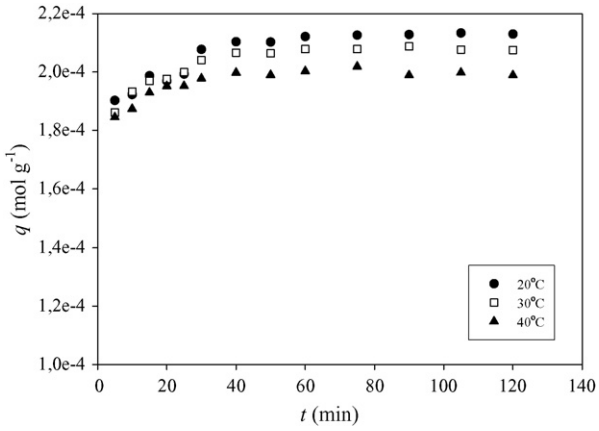

Fig. 5. Effect of contact time for the adsorption of RB19 onto DTMA–bentonite at various temperatures.

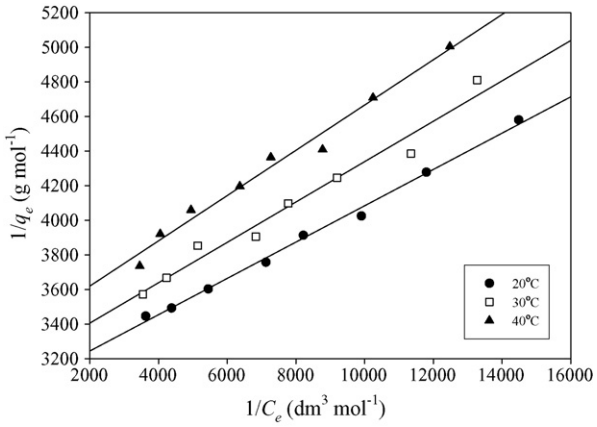

Fig. 6. Langmuir plots for the adsorption of RB19 onto DTMA–bentonite at various temperatures.

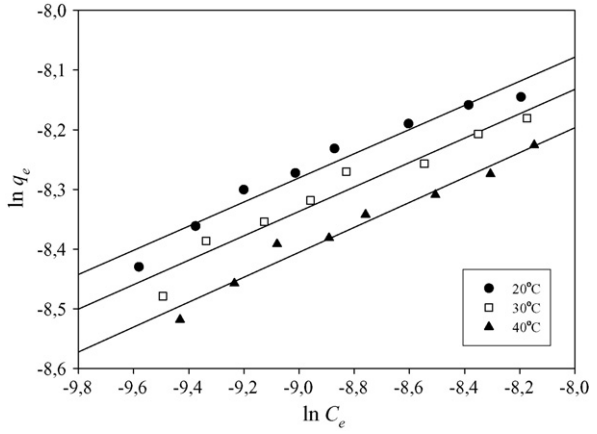

Fig. 7. Freundlich plots for the adsorption of RB19 onto DTMA–bentonite at various temperatures.

increased with contact time up to 40 min after that a maximum removal is attained. For this reason, the optimum contact time was selected as 40 min.

The equilibrium adsorption capacity of RB19 onto DTMA–bentonite decreases with increasing temperature (Fig. 5), which indicates that the adsorption of RB19 in controlled by an exothermic and physical adsorption process and due to a weakening of the attractive forces between RB19 and DTMA–bentonite sites.

Adsorption data obtained in the concentration range (2.00–4.50) $\times 10^{-4}$ mol dm^{-3} were correlated with the following linear forms of Langmuir (Eq. (1)) [31] and Freundlich (Eq. (2)) [32] adsorption isotherm models:

- Langmuir equation:

$$\frac{1}{q_e} = \frac{1}{q_{max}} + \left(\frac{1}{q_{max} K_L}\right) \frac{1}{C_e} \quad (1)$$

- Freundlich equation:

$$\ln q_e = \ln K_F + \frac{1}{n} \ln C_e \quad (2)$$

where q_e is the equilibrium dye concentration on the adsorbent (mol g^{-1}), C_e the equilibrium dye concentration in solution (mol dm^{-3}), q_{max} the monolayer capacity of the adsorbent (mol g^{-1}), K_L the Langmuir constant (dm^3 mol^{-1}) and related to the free energy of adsorption, K_F the Freundlich constant (dm^3 g^{-1}) and n (dimensionless) is the heterogeneity factor.

Best-fitted straight lines with high correlation coefficients obtained in case of Langmuir (Fig. 6) and Freundlich (Fig. 7). The all isotherm parameters derived from the respective plots are presented in Table 2. The fit of the data for RB19 adsorption onto DTMA–bentonite suggests that the Langmuir model gave slightly better fitting than that of Freundlich model, as it is obvious from a comparison of the r^2 values in Table 2. It is also evident from these data that the surface of DTMA–bentonite is made up of homogenous adsorption patches than heterogeneous adsorption patches.

The favorability of the adsorption process was confirmed by using a basic method applied by Weber and Chakravorti [33], which suggests that the linear, favorable or unfavorable nature of isotherm is dependent on the obtained value of separation factor (R_L) as unity, between 0–1 and zero, respectively. The separation factor "R_L", a dimensionless constant, can be calculated by

Table 2
Adsorption isotherm parameters for the adsorption of RB19 onto DTMA–bentonite

	t (°C)		
	20	30	40
Langmuir			
q_{max} (mol g^{-1})	3.30×10^{-4}	3.15×10^{-4}	2.98×10^{-4}
K_L (dm^3 mol^{-1})	2.89×10^4	2.72×10^4	2.57×10^4
r_L^2	0.995	0.995	0.982
R_L	7.14×10^{-2}	7.56×10^{-2}	7.97×10^{-2}
Freundlich			
n	4.946	4.896	4.793
K_F (dm^3 g^{-1})	1.56×10^{-3}	1.51×10^{-3}	1.46×10^{-3}
r_F^2	0.958	0.947	0.971

following equation:

$$R_L = \frac{1}{1 + K_L C_0} \quad (3)$$

where K_L is the Langmuir constant ($dm^3\ mol^{-1}$) and C_0 is the highest initial dye concentration ($mol\ dm^{-3}$). The values of R_L calculated as above equation (Table 2) were found less than unity at all studied temperatures, and therefore the adsorption of RB19 onto DTMA–bentonite is especially favorable at all studied temperatures.

The Freundlich constant n is a measure of the deviation from linearity of the adsorption. If a value for n is equal to unity the adsorption is linear. If a value for n is below to unity, this implies that adsorption process is chemical, but a value for n is above to unity, adsorption is favorable a physical process. The highest value of n at equilibrium is 4.946 at 20 °C, represents favorable adsorption at low temperature, and therefore this would seem to suggest that physical, which is referred the adsorption bond becomes weak and conducted with van der Waals forces, rather than chemical adsorption is dominant when it is used for adsorbing RB19.

Langmuir constant K_L can be used for calculating thermodynamic parameters, such as the change in free energy (ΔG°), enthalpy (ΔH°) and entropy (ΔS°), which are associated to the adsorption process, on the basis of the following equations:

$$\Delta G^\circ = -RT \ln K_L \quad (4)$$

$$\ln K_L = -\frac{\Delta G^\circ}{RT} = -\frac{\Delta H^\circ}{RT} + \frac{\Delta S^\circ}{R} \quad (5)$$

The plot of $\ln K_L$ as a function of $1/T$ (Fig. 8) yields a straight line from which ΔH° and ΔS° were calculated from the slope and intercept, respectively. The results of thermodynamic parameters are given in Table 3. The change of free energy for physisorption is usually between −20 and 0 kJ mol^{-1}, whereas chemisorption is a range of −80 to 400 kJ mol^{-1} [34]. The ΔG° values for the temperatures at a range of 20–40 °C were obtained between −25.04 and −26.43 kJ mol^{-1}, which indicate the nature of adsorption spontaneous. These values were in the middle of physisorption and chemisorption. It may be concluded that this is

Table 3
Thermodynamic parameters calculated from the Langmuir isotherm constant (K_L) for the adsorption of RB19 onto DTMA–bentonite

t (°C)	ΔG° (kJ mol^{-1})	ΔH° (kJ mol^{-1})	ΔS° (J K^{-1} mol^{-1})
20	−25.04		
30	−25.73	−4.55	+69.88
40	−26.43		

interpreted a physical adsorption enhanced by a chemical effect [35]. The negative value of the ΔH° (−4.55 kJ mol^{-1}) indicates that the adsorption is exothermic and the value of ΔH° implies that adsorption is also physical in nature involving weak forces of attraction. The positive value of ΔS° (+69.88 J mol^{-1} K^{-1}) corresponds to an increase in the degree of freedom of the adsorbed species.

3.3. Kinetic studies

The kinetics of adsorption data was evaluated to understand the mechanism of adsorption process by means of the pseudo-second-order kinetic and intraparticle diffusion models.

The pseudo-second-order kinetic model equation [36] can be written as follows:

$$\frac{t}{q_t} = \frac{1}{k_2 q_2^2} + \frac{1}{q_2} t \quad (6)$$

The intraparticle diffusion equation [37] is expressed as:

$$q_t = k_p t^{1/2} + C \quad (7)$$

where q_2 and q_t are the amounts of the dye adsorbed at equilibrium and at time t, in mol g^{-1}, k_2 the equilibrium rate constant of the pseudo-second-order model for the adsorption process (g mol^{-1} min^{-1}), C the intercept and k_p is the intraparticle diffusion rate constant (mol g^{-1} $min^{-1/2}$). The straight-line plots of t/q_t versus t for the pseudo-second-order (Fig. 9) and q_t against $t^{1/2}$ for the intraparticle diffusion (Fig. 10) for the adsorption of RB19 onto DTMA–bentonite have been also examined to obtain the rate parameters. All of kinetic data of RB19 under different conditions were calculated from these plots and are

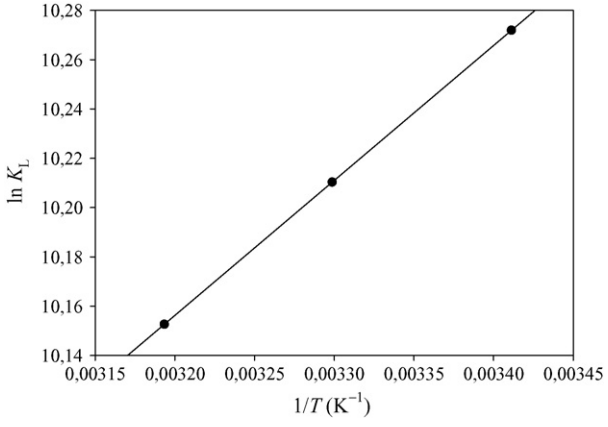

Fig. 8. Plot of $\ln K_L$ vs. $1/T$ for estimation of thermodynamic parameters for the adsorption of RB19 onto DTMA–bentonite.

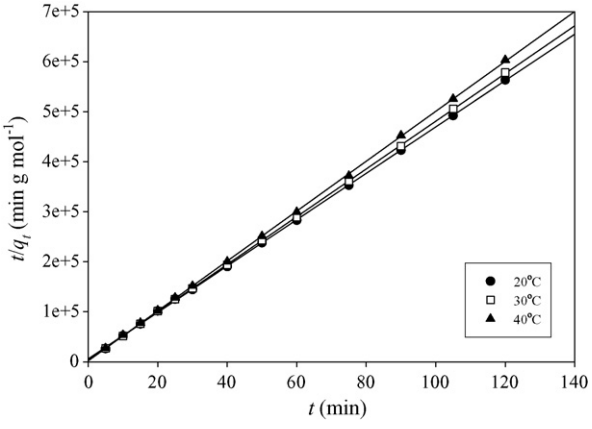

Fig. 9. Pseudo-second-order kinetic plots for the adsorption of RB19 onto DTMA–bentonite at various temperatures.

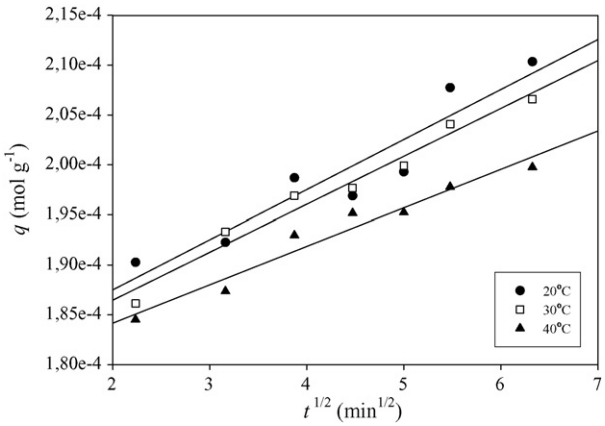

Fig. 10. Intraparticle diffusion plots for the adsorption of RB19 onto DTMA–bentonite at various temperatures.

listed in Table 4. From this table, the maximum adsorption capacities (q_2) at equilibrium are decreased from (2.16 to 2.01) $\times 10^{-4}$ mol g^{-1} for RB19 when the temperature is increased from 20 to 40 °C for DTMA–bentonite. This effect can be interpreted as assuming that a higher temperatures the total energy of the adsorbate molecules is increased and then their escaping tendency is also increased, thus, the adsorption of the adsorbate species is decreased. As a result, the adsorption process in this study favors a low temperature physical adsorption mechanism and to depend on the temperature [15,38].

The pseudo-second-order rate constants for RB19 onto DTMA–bentonite show a steady increase with solution temperature (Table 4). In generally, during a physical adsorption process, increasing temperature leads to increase the rate of approach to equilibrium, whereas decreases the equilibrium adsorption capacity [36].

As discussed above, the validity of the pseudo-second-order kinetic and intraparticle diffusion models can be quantitatively checked by using a normalized standard deviation Δq (%) calculated by the following equation [39]:

$$\Delta q\,(\%) = \sqrt{\frac{\sum [(q_{\mathrm{exp}} - q_{\mathrm{cal}})/q_{\mathrm{exp}}]^2}{n-1}} \times 100 \qquad (8)$$

Table 4
Kinetic parameters and the normalized standard deviations for the adsorption of RB19 onto DTMA–bentonite at various temperatures

	t (°C)		
	20	30	40
Pseudo-second-order			
k_2 (g mol^{-1} min^{-1})	3.60×10^3	5.65×10^3	1.15×10^3
q_2 (mol g^{-1})	2.16×10^{-4}	2.10×10^{-4}	2.01×10^{-4}
Δq (%)	1.804	1.951	0.598
r_2^2	0.999	0.999	0.999
Intraparticle diffusion			
k_p (mol g^{-1} min$^{-1/2}$)	5.02×10^{-6}	4.80×10^{-6}	3.85×10^{-6}
C	1.78×10^{-4}	1.77×10^{-4}	1.77×10^{-4}
Δq (%)	1.226	1.834	4.005
r_p^2	0.892	0.969	0.956

where n is the number of data points and the calculated results are given in Table 4. According to Table 4, the values of Δq for the best-fitted model are less than 1.952%. It is concluded that the adsorption of RB19 onto DTMA–bentonite can be best described by the pseudo-second-order kinetic model.

4. Conclusions

The research was carried out in this paper clearly suggests that surfactant-modified bentonite acts a well adsorbent for the removal of Reactive Blue 19 (RB19) from aqueous solutions. The surface modification of bentonite was tested by using the FTIR technique and elemental analysis. Batch studies suggest that the high adsorption capacity (3.30×10^{-4} mol g^{-1} or 206.58 mg g^{-1}) of DTMA–bentonite in acidic solutions (pH around 1.5) is due to the strong electrostatic interactions between its adsorption site and dye anion. The straight lines obtained for the Langmuir and Freundlich models obey to fit well with the experimental equilibrium data but the Langmuir model gives slightly better fitting than Freundlich model. The thermodynamic parameters obtained from Langmuir constant (K_L) indicate a feasible, spontaneous and exothermic adsorption. A pseudo-second-order kinetic and intraparticle diffusion models have been applied to predict the rate constants of adsorption and equilibrium adsorption capacities.

References

[1] V.K.C. Lee, J.F. Porter, G. McKay, Fixed-bed modeling for acid dye adsorption onto activated carbon, J. Chem. Technol. Biotechnol. 78 (2003) 1281–1289.
[2] S.W. Won, S.B. Choi, Y.-S. Yun, Performance and mechanism in binding of Reactive Orange 16 to various types of sludge, Biochem. Eng. J. 28 (2006) 208–214.
[3] T.N.D.C. Dantas, L.T.C. Beltrame, A.A.D. Neto, C.P.D.A. Moura, Use of microemulsions for removal of color and dyes from textile wastewater, J. Chem. Technol. Biotechnol. 79 (2004) 645–650.
[4] P. Baskaralingam, M. Pulikesi, D. Elango, V. Ramamurthi, S. Sivanesan, Adsorption of acid dye onto organobentonite, J. Hazard. Mater. 128 (2006) 138–144.
[5] A. Özcan, E.M. Öncü, A.S. Özcan, Kinetics, isotherm and thermodynamic studies of adsorption of Acid Blue 193 from aqueous solutions onto natural sepiolite, Colloids Surf. A: Physicochem. Eng. Aspects 277 (2006) 90–97.
[6] A. Özcan, E.M. Öncü, A.S. Özcan, Adsorption of Acid Blue 193 from aqueous solutions onto DEDMA-sepiolite, J. Hazard. Mater. 129 (2006) 244–252.
[7] K. Ravikumar, B. Deebika, K. Balu, Decolourization of aqueous dye solutions by a novel adsorbent: application of statistical designs and surface plots for the optimization and regression analysis, J. Hazard. Mater. 122 (2005) 75–83.
[8] K. Ravikumar, K. Pakshirajan, T. Swaminathan, K. Balu, Optimization of batch process parameters using response surface methodology for dye removal by a novel adsorbent, Chem. Eng. J. 105 (2005) 131–138.
[9] V.K. Gupta, I. Ali, Suhas, D. Mohan, Equilibrium uptake and sorption dynamics for the removal of a basic dye (basic red) using low-cost adsorbents, J. Colloid Interf. Sci. 265 (2003) 257–264.
[10] V.K. Gupta, A. Mittal, L. Krishnan, V. Gajbe, Adsorption kinetics and column operations for the removal and recovery of malachite green from wastewater using bottom ash, Sep. Purif. Technol. 40 (2004) 87–96.
[11] A. Mittal, L. Kurup Krishnan, V.K. Gupta, Use of waste materials-bottom ash and de-oiled soya, as potential adsorbents for the removal of amaranth from aqueous solutions, J. Hazard. Mater. 117 (2005) 171–178.

[12] A. Mittal, Use of hen feathers as potential adsorbent for the removal of a hazardous dye, Brilliant Blue FCF, from wastewater, J. Hazard. Mater. 128 (2006) 233–239.
[13] K.G. Bhattacharyya, A. Sharma, Azadirachta indica leaf powder as an effective biosorbent for dyes: a case study with aqueous Congo Red solutions, J. Environ. Manage. 71 (2004) 217–229.
[14] A.S. Özcan, B. Erdem, A. Özcan, Adsorption of Acid Blue 193 from aqueous solutions onto BTMA–bentonite, Colloids Surf. A: Physicochem. Eng. Aspects 266 (2005) 73–81.
[15] A.S. Özcan, B. Erdem, A. Özcan, Adsorption of Acid Blue 193 from aqueous solutions onto Na–bentonite and DTMA–bentonite, J. Colloid Interf. Sci. 280 (2004) 44–54.
[16] A.S. Ozcan, S. Tetik, A. Ozcan, Adsorption of acid dyes from aqueous solutions onto sepiolite, Sep. Sci. Technol. 39 (2004) 301–320.
[17] B. Armagan, O. Ozdemir, M. Turan, M.S. Çelik, The removal of reactive azodyes by natural and modified zeolites, J. Chem. Technol. Biotechnol. 78 (2003) 725–732.
[18] B. Armağan, M. Turan, M.S. Çelik, Equilibrium studies on the adsorption of reactive azodyes into zeolite, Desalination 170 (2004) 33–39.
[19] Y.E. Benkli, M.F. Can, M. Turan, M.S. Çelik, Modification of organozeolite surface for the removal of reactive azodyes in fixed-bed reactors, Water Res. 39 (2005) 487–493.
[20] S. Wang, H. Li, L. Xu, Application of zeolite MCM-22 for basic dye removal from wastewater, J. Colloid Interf. Sci. 295 (2006) 71–78.
[21] C.-C. Wang, L.-C. Juang, T.-C. Hsu, C.-K. Lee, J.-F. Lee, F.-C. Huang, Adsorption of basic dyes onto montmorillonite, J. Colloid Interf. Sci. 273 (2004) 80–86.
[22] R. Wibulswas, Batch and fixed bed sorption of methylene blue on precursor and QACs modified montmorillonite, Sep. Purif. Technol. 39 (2004) 3–12.
[23] T. Polubesova, M. Epstein, S. Yariv, I. Lapides, S. Nir, Adsorption of alizarinate-micelle complexes on Na-montmorillonite, Appl. Clay Sci. 24 (2004) 177–183.
[24] M. Ogawa, R. Kawai, K. Kuroda, Adsorption and aggregation of a cationic cyanine dye on smectites, J. Phys. Chem. (US) 100 (1996) 16218–16221.
[25] F.L. Arbeloa, J.M. Herran Martinez, T.L. Arbeloa, I.L. Arbeloa, Hydrophobic effect on the adsorption of rhodamines in aqueous suspensions of smectites. The rhodamine 3B/Laponite B system, Langmuir 14 (1998) 4566–4573.
[26] A. Czímerová, J. Bujdák, A. Gáplovský, The aggregation of thionine and methylene blue dye in smectite dispersion, Colloids Surf. A: Physicochem. Eng. Aspects 243 (2004) 89–96.
[27] Q.H. Hu, S.Z. Qiao, F. Haghseresht, M.A. Wilson, G.Q. Lu, Adsorption study for removal of basic red dye using bentonite, Ind. Eng. Chem. Res. 45 (2006) 733–738.
[28] S. Al-Asheh, F. Banat, L. Abu-Aitah, The removal of methylene blue dye from aqueous solutions using activated and non-activated bentonites, Ads. Sci. Technol. 21 (2003) 451–462.
[29] Y.-H. Shen, Preparation of organobentonite using non-ionic surfactants, Chemosphere 44 (2001) 989–995.
[30] G. Sheng, S. Xu, S.A. Boyd, Cosorption of organic contaminants from water by hexadecyltrimethylammonium-exchanged clays, Water Res. 30 (1996) 1483–1489.
[31] I. Langmuir, The adsorption of gases on plane surfaces of glass, mica and platinum, J. Am. Chem. Soc. 40 (1918) 1361–1403.
[32] H.M.F. Freundlich, Über die adsorption in lösungen, Z. Phys. Chem. 57 (1906) 385–470.
[33] T.W. Weber, R.K. Chakravorti, Pore and solid diffusion models for fixed-bed adsorbers, J. Am. Inst. Chem. Eng. 20 (1974) 228–238.
[34] M.J. Jaycock, G.D. Parfitt, Chemistry of Interfaces, Ellis Horwood Ltd., Onichester, 1981.
[35] Y. Yu, Y.-Y. Zhuang, Z.-H. Wangy, Adsorption of water-soluble dye onto functionalized resin, J. Colloid Interf. Sci. 242 (2001) 288–293.
[36] Y.S. Ho, G. McKay, Sorption of dye from aqueous solution by peat, Chem. Eng. J. 70 (1998) 115–124.
[37] W.J. Weber Jr., J.C. Morriss, Kinetics of adsorption on carbon from solution, J. Sanitary Eng. Div. Am. Soc. Civil Eng. 89 (1963) 31–60.
[38] Y.S. Ho, G. McKay, Kinetic models for the sorption of dye from aqueous solution by wood, Process Saf. Environ. Protect. 76 (1998) 183–191.
[39] F.-C. Wu, R.-L. Tseng, R.-S. Juang, Kinetic modeling of liquid-phase adsorption of reactive dyes and metal ions on chitosan, Water Res. 35 (2001) 613–618.